INL/CON-26-93385

An FMEA-Informed Reliability Framework for Infinitely Variable Transmissions in Tidal Energy Systems

Wen-Chi Cheng[a], Fazlur Rahman Bin Karim[b,e], Gang Li[c], Mucun Sun[d]

[a]Idaho National Laboratory, Idaho Falls, Idaho, USA, wenchi.cheng@inl.gov

[b]Idaho National Laboratory, Idaho Falls, Idaho, USA, fazlurrahmanbin.karim@inl.gov

[c]Hall School of Mechanical Engineering, Mississippi State University, Starkville, Mississippi, USA, gli@me.msstate.edu

[d]Idaho National Laboratory, Idaho Falls, Idaho, USA, Mucun.Sun@inl.gov

[e]The University of Texas at Dallas, Richardson, Texas, USA,

Abstract

Tidal current energy converters (TCECs) are a promising source of predictable renewable energy, but their commercial deployment depends on the reliability of drivetrain components operating in harsh subsea environments. Infinitely variable transmissions (IVTs) are attractive for TCEC applications because they can continuously adjust speed ratios under high-torque, low-speed operating conditions using all-gear contact, thereby improving energy-capture performance while avoiding the sliding losses associated with friction-based continuously variable transmissions. However, the reliability of IVTs in tidal applications has received limited attention, and a structured assessment is needed to support technology qualification and future commercialization.

This paper presents a failure mode and effects analysis (FMEA)-informed reliability framework for the IVT gearbox in a TCEC system. The gearbox is decomposed into five functional component groups: a non-circular gear pair for speed modulation, planetary gear sets for speed combining and control, rack-pinion sets for motion conversion, output gears for final torque delivery, and the gearbox seal for environmental isolation. Each component group is evaluated with respect to failure modes and mechanisms associated with subsea operation, including cyclic loading, abrasive contamination, corrosion, biofouling, debris-induced scuffing, and water ingress.

The FMEA follows a systematic seven-step process covering component specification, process-function definition, failure-mode identification, failure-mechanism analysis, risk scoring, risk-priority-number (RPN) ranking, and mitigation strategy development. Severity, frequency, and detectability scores are assigned using the Gearbox Reliability Database, literature-based evidence, and engineering judgment to reflect the limited experimental data currently available for this IVT design. The analysis identifies root bending fatigue as the dominant design-critical failure mechanism across multiple gear components, with the highest RPN values occurring in the non-circular gear pair and planetary gear sets. Additional important mechanisms include abrasive and corrosive wear, debris-induced scuffing, edge loading, and seal degradation.

The FMEA results are then combined with literature-derived failure-rate estimates and a probabilistic physics-of-failure estimate for the non-circular gear pair to support a component-level reliability assessment. For the non-repairable case, the IVT gearbox is modeled as a series system composed of the planetary gear, non-circular gear, rack-pinion gear, output gear, and gearbox seal. Baseline one-year reliability is calculated using midpoint failure-rate estimates, and a one-at-a-time sensitivity analysis is performed using lower- and upper-bound failure-rate values. The sensitivity results identify the gearbox seal, planetary gear, and non-circular gear as the primary contributors to uncertainty in overall IVT gearbox reliability. This framework provides a structured basis for IVT reliability qualification and identifies the data-collection, monitoring, and design-improvement priorities needed to support TCEC commercialization.

1 Introduction

Tidal current energy converters (TCECs) require gear transmissions to convert the high-torque, low-speed rotation of turbine blades, typically 5–7 r/min, into the higher rated speeds required by generators. This conversion can require speed ratios as high as 1:150 [1]. While conventional multistage planetary gearboxes are commonly used, their fixed gear ratios can amplify speed fluctuations caused by tidal turbulence, increasing generator stress and potentially contributing to system failures. Advanced technologies such as infinitely variable transmissions (IVTs) are being developed to provide continuously variable speed ratios using all-gear contact, allowing TCECs to maintain efficient energy harvesting under variable flow conditions.

Originally developed for wind-turbine applications [2], IVTs have recently been adapted for TCECs because they can produce a nearly constant output speed from a variable input speed [3]. However, the IVT system differs substantially from conventional wind-turbine gearboxes, and gearboxes have a long history of reliability challenges in wind-energy applications [4]. Existing IVT research for TCECs has primarily focused on speed and transmission control, while reliability assessment has received limited attention despite being a critical step in technology qualification and commercialization.

Unlike wind-turbine gearboxes, IVTs deployed in tidal environments are exposed to additional degradation mechanisms associated with seawater, corrosion, biofouling, and abrasive particles. Additional sub-failure modes may therefore be present relative to wind-turbine gearbox applications. In this paper, we first examine the main gear components of the IVT for TCEC applications and then perform a failure mode and effects analysis (FMEA). The FMEA results are used to support the development of a reliability model and to identify future research needs for reducing uncertainty in the IVT design.

2 Infinitely Variable Transmission in Tidal Energy Converters

The IVT in a TCEC is a specialized mechanical system designed to convert variable-speed hydrokinetic energy from a tidal turbine into a stable rotational output for an electrical generator [5, 6]. The TCEC/IVT layout used for flume-flow testing is shown in Fig. 1. Unlike friction-based continuously variable transmissions (CVTs), the IVT uses all-gear contact rather than frictional contact, allowing it to handle the high-torque, low-speed conditions typical of subsea environments without the sliding power losses associated with CVTs.

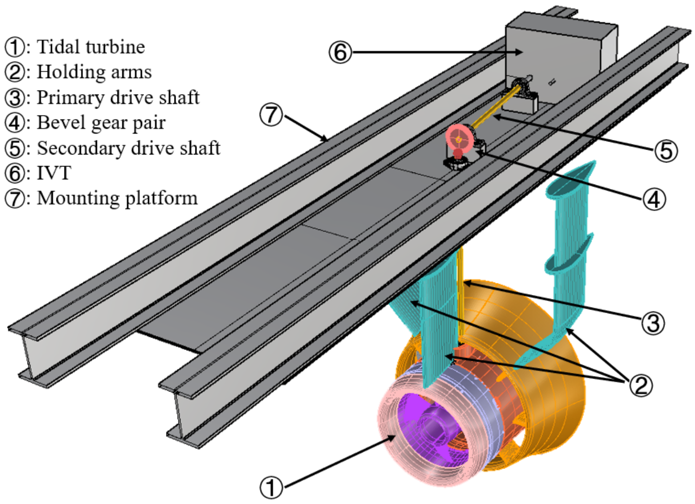

Figure 1: Layout of the TCEC, including a tidal turbine, a bevel gear pair, and the IVT.

The IVT is composed of a non-circular gear pair that modulates the input speed, an input-control module that combines the modulated speed with a control input using planetary gear sets, and a motion-conversion module that employs scotch-yoke systems and rack-pinion sets to achieve a continuously variable speed ratio and a nearly constant output speed. The schematic of the IVT is shown in Fig. 2. The operation of the IVT occurs through the following stages:

(1) *Speed modulation via non-circular gears (NCG):* The process begins as the turbine's variable rotation enters the IVT through a non-circular gear pair [7]. Because the downstream mechanical components naturally generate sinusoidal speed variations, the NCG is designed with an asymmetrical pitch profile to instantaneously modulate the input speed and reduce these inherent fluctuations.

(2) *Power merging in the input-control module (ICM):* The modulated speed enters the ICM and is transmitted to the carriers of two planetary gear sets. Simultaneously, a stepper motor provides a prescribed control speed to the sun gears of these sets. The planetary gear sets combine the modulated turbine speed with the control speed and deliver a merged rotational speed through their ring gears.

(3) *Motion conversion and ratio adjustment:* The merged speeds drive the motion-conversion module (MCM), which uses two scotch-yoke systems (SYSs). These SYSs convert rotational motion into the translational, or reciprocating, motion of the yokes. The core functionality of the IVT lies in its adjustable crank length; by using the control speed to change this length, the transmission can continuously vary its speed ratio from zero to a specified maximum. This capability allows the TCEC to maintain its optimal tip-speed ratio (TSR) across cut-in and rated tidal-current speeds.

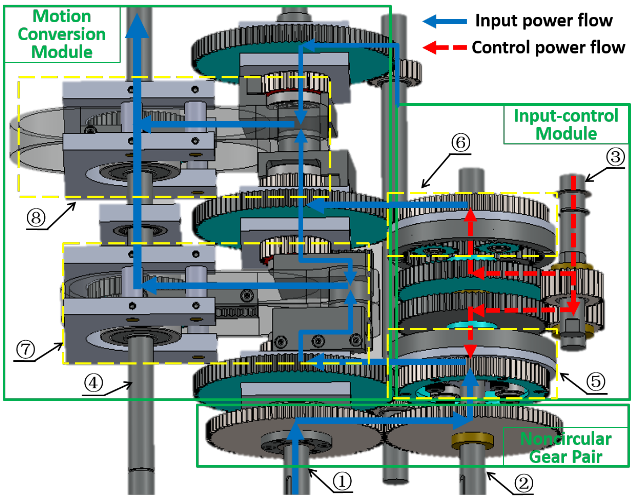

Figure 2: Schematic drawing of the IVT [5], where 1 is the input shaft, 2 is the secondary shaft, 3 is the control shaft, 4 is the output shaft, 5 is the first planetary gear set (PGS), 6 is the second PGS, 7 is the first scotch-yoke system (SYS), and 8 is the second SYS.

To ensure effective operation of the IVT for TCECs, the system can incorporate model-based closed-loop speed-ratio control and time-delay feedback control [8], or data-driven speed control [9]. These control systems track desired output speeds and adjust the crank length in real time to compensate for disturbances such as water turbulence and response lags in the mechanical drivetrain.

3 Failure Mode and Effects Analysis

FMEA is widely used in system reliability analysis [10] to identify critical failure modes and the underlying mechanisms that contribute to them in newly designed systems. Although the specific FMEA tasks may vary depending on system complexity and analysis objectives, the process generally follows the steps shown in Fig. 3.

For Step 1, the FMEA scope is defined based on the target system and components. In this study, the IVT gearbox is selected as the target system. It includes a non-circular gear pair, planetary gear systems, and a motion-conversion module, as shown in Fig. 2. In Step 2, the process function is defined as the intended function of each gear component that could be affected by failure. In Step 3, failure modes associated with each component are identified to determine what can fail within each function. In Step 4,

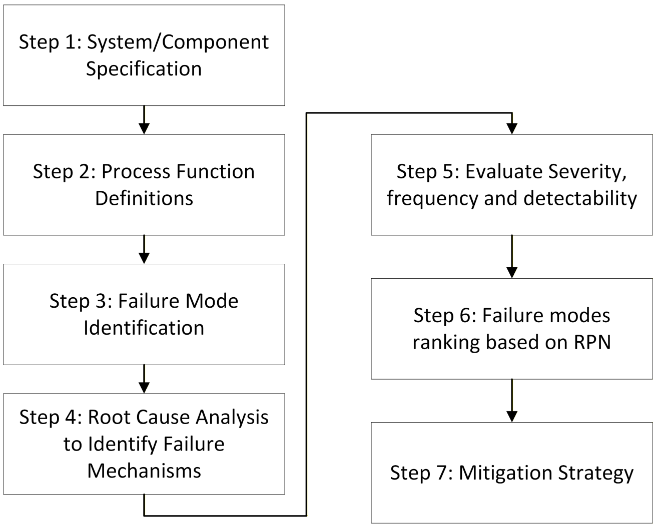

Figure 3: Methodological steps for performing FMEA.

the underlying failure mechanisms leading to each failure mode are identified.

In Step 5, scores from one to ten are assigned for severity, frequency, and detectability. Severity represents the consequence of the failure, where one is the least severe and ten is the most severe. Frequency represents how often the failure is expected to occur, where one is rare and ten is very frequent. Detectability represents how easily the failure can be identified, where one is very easy to detect and ten is extremely difficult to detect. For each failure event, a risk priority number (RPN) is evaluated by multiplying severity (S), frequency (F), and detectability (D). In Step 6, failure modes are ranked based on RPN, with the highest RPN indicating the highest priority. In Step 7, which is added to support the IVT design phase, mitigation strategies are proposed to improve the design or operation for each failure scenario.

4 FMEA Results and Discussions

As shown in Fig. 3, several FMEA steps, especially Step 6, require substantial failure or testing data. However, the IVT for TCEC applications is still in the design phase, where limited experimental data and few directly applicable failure databases are available. Therefore, the authors first investigated the Gearbox Reliability Database [3], which records failure modes and root causes for wind-turbine gearboxes, and supplemented this information with engineering judgment based on the mechanical and physical constraints of subsea IVT operation. Because the IVT would ultimately be deployed subsea, water ingress or silt abrasion could cause degradation that affects the entire system. Table 1 integrates the failure-mode/root-cause mapping with the RPN scores and mitigation strategies for each identified failure mechanism.

Table 1: Integrated FMEA table for IVT gearboxes. Component score is calculated as the mean RPN across the failure mechanisms assigned to each component.

Fail. ID	**Process Function**	**Failure Mode**	**Failure Mechanism**	**RPN (S×F×D)**	**Mitigation Strategy**
A. Non-circular gear pair – component score (mean RPN) = 206.0; maximum RPN = 320					
A.1	Transmit input torque and create modulated speed	Loss of torque transmission	Root bending fatigue	320 (10×4×8)	Increase root strength (fillet, case depth); reduce torque spikes; vibration monitoring for crack detection.
A.2	Transmit input torque and create modulated speed	Excessive vibration/noise	Micro-pitting causing increased surface roughness and transmission error	98 (7×7×2)	Increase film thickness; improve surface finish; reduce dwell; monitor vibration and oil condition.

Continued on next page

Table 1 continued from previous page					
Fail. ID	**Process Function**	**Failure Mode**	**Failure Mechanism**	**RPN (S×F×D)**	**Mitigation Strategy**
A.3	Transmit input torque and create modulated speed	Loss of modulation accuracy	Fretting wear at hub-shaft interface	200 (8×5×5)	Specify interference fits; apply anti-fretting coatings; limit micro-motion; monitor modulation accuracy.
B. Planetary gear sets – component score (mean RPN) = 159.1; maximum RPN = 320					
B.1	Combine control speed and modulated speed	Loss of combined-speed accuracy	Sun gear tooth deflection under load	216 (9×3×8)	Increase sun tooth stiffness; improve load sharing; manage transients; monitor transmission error trends.
B.2	Combine control speed and modulated speed	Loss of combined-speed accuracy	Abrasive flank wear	175 (7×5×5)	Improve filtration; use hardened surfaces; maintain lubricant quality; monitor backlash and debris trends.
B.3	Combine control speed and modulated speed	Loss of torque transmission	Root bending fatigue of planet gear teeth	320 (10×4×8)	Strengthen planet tooth root; improve load sharing; limit transients; monitor vibration for crack initiation.
B.4	Combine control speed and modulated speed	Loss of torque transmission	Ring gear rim/web cracking	160 (10×2×8)	Avoid thin-rim designs; improve fillet geometry; control deflection; conduct periodic NDE for cracks.
B.5	Combine control speed and modulated speed	Excessive vibration/noise	Subsurface fatigue leading to macro-pitting and debris formation	96 (8×4×3)	Improve contact stress margin; optimize geometry; maintain lubricant; vibration and debris trending.
B.6	Combine control speed and modulated speed	Excessive vibration/noise	Micropitting → macropitting progression	120 (8×5×3)	Increase film thickness; superfinish surfaces; maintain lubricant; early vibration and debris alarms.
B.7	Combine control speed and modulated speed	Overheating	Edge loading leading to localized heating	162 (9×3×6)	Correct misalignment; apply tooth modifications; ensure oil delivery; monitor temperature and load correlation.
B.8	Combine control speed and modulated speed	Overheating	Micropitting/scuffing increasing friction coefficient	96 (8×4×3)	Reduce friction losses via finish and viscosity; manage duty; monitor temperature-torque correlation.
B.9	Combine control speed and modulated speed	Locked rotation	Scuffing due to film collapse	120 (10×2×6)	Maintain film thickness; use scuff-resistant coatings; controlled ramps; fast thermal shutdown logic.
B.10	Combine control speed and modulated speed	Locked rotation	Debris-induced scuffing event	126 (9×2×7)	Install magnets and filters; maintain cleanliness; prevent bypass; monitor debris with rapid shutdown.
C. Rack–pinion sets – component score (mean RPN) = 167.8; maximum RPN = 210					
C.1	Convert translation (yoke) to rotation	Excess backlash	Abrasive wear of rack and pinion teeth	210 (6×7×5)	Upgrade filtration; use wear-resistant coatings; maintain alignment; monitor backlash and particle counts.
C.2	Convert translation (yoke) to rotation	Fail-to-run	Debris wedging in engagement	189 (9×3×7)	Install debris guards, magnets, filters; maintain cleanliness; use debris sensors with shutdown logic.
C.3	Convert translation (yoke) to rotation	Tooth chipping	Impact loading at reversal leading to stress concentration	144 (8×3×6)	Apply tip chamfers; control reversal dynamics; increase tooth toughness; monitor impact signatures.
C.4	Convert translation (yoke) to rotation	Overheating	Boundary lubrication loss	128 (8×4×4)	Ensure lubrication at low speed; select suitable lubricant; manage loads; monitor temperature.
C.5	Convert translation (yoke) to rotation	Corrosion-driven degradation	Corrosive wear	168 (6×4×7)	Enhance sealing; use corrosion inhibitors; install water sensors; apply protective coatings.
D. Output gears – component score (mean RPN) = 176.7; maximum RPN = 240					
D.1	Provide rotational outputs	Loss of output torque contribution	Root bending fatigue of output gear teeth	240 (10×3×8)	Increase root strength; limit shock loads; alignment control; crack monitoring with periodic NDE inspection.
D.2	Provide rotational outputs	Excessive vibration/noise	Subsurface fatigue leading to spall formation	140 (7×4×5)	Improve surface finish; control contact stress; maintain cleanliness; monitor vibration and debris.

Continued on next page

Table 1 continued from previous page					
Fail. ID	**Process Function**	**Failure Mode**	**Failure Mechanism**	**RPN (S×F×D)**	**Mitigation Strategy**
D.3	Provide rotational outputs	Efficiency loss	Profile wear increasing sliding losses	150 (5×5×6)	Control contamination; use wear-resistant surfaces; maintain lubricant; monitor efficiency and temperature trends.
E. Gearbox seal – component score (mean RPN) = 144.0; maximum RPN = 144					
E.1	Isolate seawater from equipment	Water ingress beyond limit	Seal degradation (lip wear, elastomer aging, extrusion, pressure differential)	144 (9×4×4)	Install dual seals with backup rings; pressure compensation; water-in-oil monitoring; preventive seal replacement.

As shown in Table 1, the target IVT gearbox is decomposed into five major component groups: the non-circular gear pair, planetary gear sets, rack-pinion sets, output gears, and gearbox seal. Common failure modes include loss of torque transmission, excessive vibration, overheating, backlash, and water ingress. Root bending fatigue is identified as a critical failure mechanism because it contributes to multiple high-RPN failure modes across gear components. Other mechanisms, including abrasive wear, corrosive wear, fretting wear, and profile wear, appear in different forms depending on component location and contact conditions.

A component-level FMEA score was calculated as the mean RPN of all failure mechanisms assigned to the same component. This approach avoids automatically assigning a higher score to components with more listed mechanisms. The resulting component scores are A = 206.0, B = 159.1, C = 167.8, D = 176.7, and E = 144.0. The corresponding maximum single-mechanism RPN values are A = 320, B = 320, C = 210, D = 240, and E = 144, indicating that the non-circular gear pair and planetary gear sets contain the highest-priority individual failure mechanisms.

When gear failure data are available, severity, frequency, and detectability scores can be defined based on investigation reports or maintenance records. However, because testing data for this new IVT design are limited, subject-matter expert (SME) input is used to support the FMEA scoring. A rubric for evaluating severity, frequency, and detectability is shown in Table 2.

Table 2: Unified rubric for severity (S), frequency (F), and detectability difficulty (D).

Metric	**Score**	**Definition**
S	1–2	No or negligible impact on performance
	3–6	Degraded or minor impact on performance
	7–8	Derated operation or major impact on performance
	9–10	Forced outage or catastrophic shutdown
F	1–2	Rare
	3–4	Occasional
	5–6	Moderate
	7–8	Frequent
	9–10	Very frequent
D	1–2	Very easy to detect early
	3–4	Easy to detect with common sensors
	5–6	Moderate detectability
	7–8	Difficult to detect
	9–10	Extremely difficult to detect

Based on the evaluation rubric, the RPN values in Table 1 rank the failure sequences and connect each mechanism directly to a mitigation strategy. The most important failure mechanisms are root bending fatigue of the non-circular gear pair and planet gear teeth, each with an RPN of 320. These results indicate that detailed load evaluation is necessary for ensuring gearbox reliability. Among the mitigation strategies, increasing the tooth-root safety margin or strength remains the key design step, highlighting the importance of evaluating uncertainty in both gear loading and material strength. A detailed probabilistic physics-of-failure analysis for root bending fatigue of the IVT non-circular gear pair is provided in [11].

5 FMEA-Informed Reliability Assessment

Although FMEA provides risk priorities and supports mitigation planning, it does not directly quantify IVT reliability. This section develops a reliability assessment for the IVT gearbox based on the FMEA results, relevant literature, and simulation outputs, assuming that the IVT is a non-repairable system [10].

5.1 Data Collection for Reliability Assessment

The FMEA results identify five functional component groups that contribute to IVT risk: the non-circular gear, planetary gear, rack-pinion gear, output gear, and gearbox seal.

Failure rates for the planetary gear, rack-pinion gear, output gear, and gearbox seal were obtained from available literature based on their respective application domains. The failure-rate estimate for the non-circular gear pair was obtained using a probabilistic physics-of-failure analysis [11].

Due to the limited availability of direct component-level failure-rate data for IVT gearboxes operating in tidal energy systems, relevant reliability information was sourced from analogous applications. Failure-rate data from offshore wind-turbine applications were prioritized because of their closer mechanical, operational, and environmental similarities to the tidal-energy domain [12, 13, 14, 15, 16]. Similar drivetrain components are also widely used in wind-energy systems, making wind-energy reliability data a suitable basis for estimating component failure behavior.

Given the variability in reported failure-rate data across operating environments, load conditions, and maintenance practices, each component was assigned lower-, midpoint-, and upper-bound failure-rate estimates reflecting values documented in the literature. Table 3 summarizes these failure-rate estimates and the corresponding one-year reliability values for the key IVT gearbox components considered in this study. Because the extracted failure-rate data are predominantly reported as point estimates rather than statistical distributions, the values adopted in this study represent the best available deterministic estimates of component failure behavior derived from the literature.

Table 3: Failure-rate and corresponding reliability estimates for key IVT gearbox components.

Component	λ (failures/year)			$R(t)$ (%, $t = 1$ year)		
	Lower	**Mid**	**Upper**	**Upper**	**Mid**	**Lower**
Planetary Gear	0.000189	0.0500	0.1500	99.98	95.23	86.07
Non-Circular Gear	0.0200	0.0500	0.1452	97.15	92.88	86.49
Rack-Pinion Gear	0.0040	0.0080	0.0200	99.60	99.20	98.00
Output Gear	0.0020	0.0600	0.1000	98.00	94.18	90.50
Gearbox Seal	0.0300	0.0739	0.1892	97.00	92.88	82.76

The IVT gearbox is modeled as a series system in which the failure of any individual component results in failure of the entire gearbox [17]. One benefit of this series subsystem configuration is that each subsystem can be modeled independently without explicitly modeling common-cause failure (CCF), because a single component failure is sufficient to cause system failure. However, without redundancy, a major failure in any IVT module causes a full system shutdown. Depending on the target reliability, designers may consider adding redundancy to improve overall IVT performance.

Assuming statistically independent component failures, the overall reliability of the IVT gearbox can be expressed as the product of the reliabilities of its constituent components:

$$R_{\mathrm{IVT}}(t) = R_{\mathrm{PG}}(t) \times R_{\mathrm{NCG}}(t) \times R_{\mathrm{RPG}}(t) \times R_{\mathrm{OG}}(t) \times R_{\mathrm{GS}}(t) \quad (1)$$

where $R_{PG}(t)$, $R_{NCG}(t)$, $R_{RPG}(t)$, $R_{OG}(t)$, and $R_{GS}(t)$ are the reliabilities of the planetary gear, non-circular gear, rack-pinion gear, output gear, and gearbox seal, respectively.

Each component is assumed to follow an exponential reliability model with a constant failure rate. Accordingly, the reliability of the ith component is calculated as:

$$R_i(t) = e^{-\lambda_i t} \tag{2}$$

where λ_i is the component failure rate in failures per year and t is the mission time. Combining Equations (1) and (2) gives:

$$R_{IVT}(t) = \exp\left[-(\lambda_{PG} + \lambda_{NCG} + \lambda_{RPG} + \lambda_{OG} + \lambda_{GS})t\right] \tag{3}$$

where λ_{PG}, λ_{NCG}, λ_{RPG}, λ_{OG}, and λ_{GS} denote the failure rates of the planetary gear, non-circular gear, rack-pinion gear, output gear, and gearbox seal, respectively. The baseline reliability values were calculated using the midpoint reliability estimate for each component. Under the series-system assumption, the baseline reliability of the IVT gearbox was obtained by multiplying the midpoint reliability values of all constituent components according to Equation (1). This baseline serves as the reference condition for the sensitivity analysis, while the lower- and upper-bound reliability values are used to evaluate the influence of component failure-rate uncertainty on the overall IVT gearbox reliability assessment.

5.2 Reliability Sensitivity Analysis

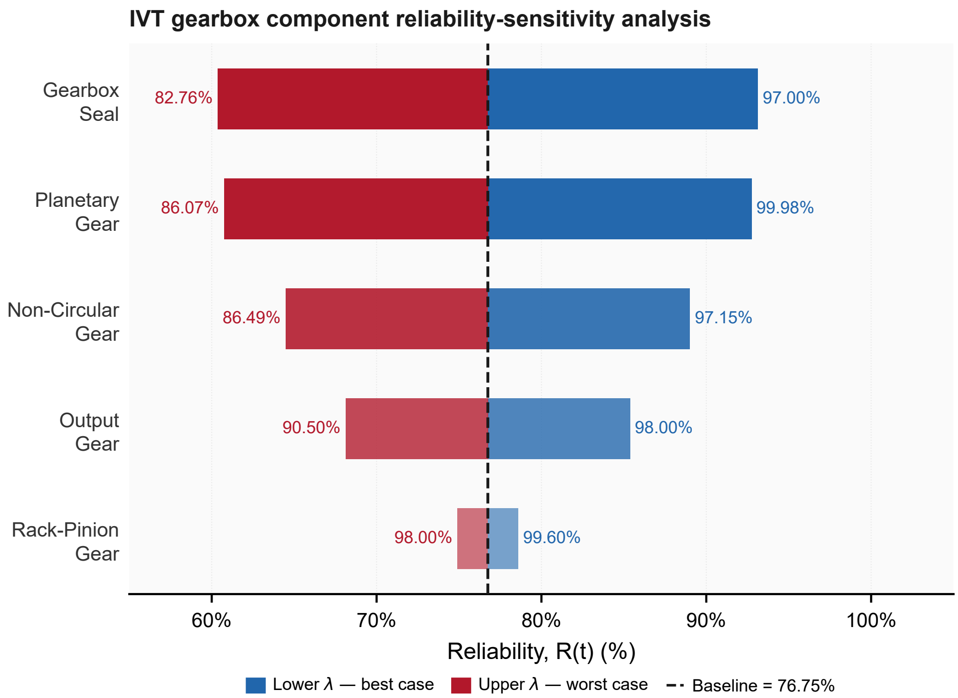

Figure 4: One-at-a-time sensitivity analysis of IVT gearbox component reliability over a one-year mission period. The dashed line indicates the baseline system reliability (76.75%); blue and red bars represent the lower- and upper-bound failure-rate cases, respectively.

Figure 4 presents the results of the one-at-a-time (OAT) sensitivity analysis in the form of a tornado diagram. The dashed vertical line represents the baseline IVT gearbox reliability of 76.75%. For each component, the blue bar corresponds to the best-case scenario, while the red bar represents the worst-case scenario. The length of each bar reflects the magnitude of reliability variation caused by uncertainty in the corresponding component failure rate.

The diagram shows that the gearbox seal is the dominant contributor to reliability uncertainty within the IVT gearbox system. The one-year reliability of this component varies from 82.76% under the upper-bound failure-rate assumption to 97.00% under the lower-bound failure-rate assumption, resulting in the largest uncertainty range among all components. This result highlights the critical role of sealing systems in preventing lubricant loss, contamination ingress, and secondary drivetrain failures.

The planetary gear is the second most influential component, with reliability ranging from 86.07% to 99.98%. Similar behavior is observed for the non-circular gear, whose reliability varies between 86.49% and 97.15%. The relatively large uncertainty ranges associated with both components indicate that improvements in their reliability characterization would significantly reduce uncertainty in the overall IVT gearbox reliability assessment.

The output gear exhibits moderate sensitivity, with reliability values ranging from 90.50% to 98.00%. Although the uncertainty range is smaller than those of the planetary gear, gearbox seal, and non-circular gear, the output gear remains an important reliability contributor because of its critical role in torque transmission within the drivetrain system.

Overall, the sensitivity analysis identifies the gearbox seal, planetary gear, and non-circular gear as the primary contributors to reliability uncertainty within the IVT gearbox. These components should therefore be prioritized for future reliability data collection, condition monitoring, design improvement, and maintenance optimization. Reducing uncertainty in these components is expected to yield the greatest improvement in confidence associated with the overall IVT gearbox reliability assessment.

6 Conclusions

A new infinitely variable transmission (IVT) has been developed for a tidal current energy converter (TCEC). The main feature of the IVT is its ability to provide a continuously variable speed ratio using all-gear contact, thereby supporting effective operation under variable flow-speed conditions. The IVT gearbox includes a non-circular gear pair, planetary gear sets, rack-pinion sets, output gears, and the gearbox seal.

A systematic FMEA was performed to identify potential failure modes and underlying failure mechanisms for the IVT. Root bending fatigue was identified as the dominant design-critical failure mechanism, contributing to multiple high-priority failure modes across different gear components. The FMEA results also informed the development of a reliability model that incorporates multiple sources of relevant data, including literature-derived failure-rate estimates and a probabilistic physics-of-failure estimate for the non-circular gear pair.

A sensitivity analysis of the FMEA-informed reliability model identified the gearbox seal, planetary gear, and non-circular gear as the primary contributors to uncertainty in one-year IVT gearbox reliability. These results indicate that future data collection and monitoring should prioritize seal performance, planetary gear reliability, and non-circular gear tooth-root strength.

Future research will focus on experimental testing of the IVT to reduce uncertainty in component failure-rate estimates and improve confidence in reliability predictions. This work represents an important step toward qualifying IVT technology for TCEC systems and other marine-power applications.

Acknowledgments

This manuscript has been authored by Battelle Energy Alliance, LLC under Contract No. DE-AC07-05ID14517 with the U.S. Department of Energy. This work was supported through the U.S. Department of Energy Water Power Technologies Office's Testing Expertise and Access for Marine Energy Research (TEAMER) program. The second author acknowledges financial support from the National Science Foundation under Grant No. 2329791.

References

[1] Gang Li and Weidong Zhu. A review on up-to-date gearbox technologies and maintenance of tidal current energy converters. *Energies*, 15(23):9236, 2022.

[2] Xuefeng Wang. *Design, Modeling, Analysis, Control and Testing of an Infinitely Variable Transmission*. University of Maryland, Baltimore County, 2017.

[3] Francisco Oyague, D Gorman, and Shuangwen Sheng. Nrel gearbox reliability collaborative experimental data overview and analysis. Technical report, National Renewable Energy Laboratory (NREL), Golden, CO (United States), 2010.

[4] Gang Li and Weidong Zhu. Time-delay closed-loop control of an infinitely variable transmission system for tidal current energy converters. *Renewable Energy*, 189:1120–1132, 2022.

[5] Gang Li and Weidong Zhu. Control and flume flow experiments of a tidal current energy converter with an infinitely variable transmission. *IEEE/ASME Transactions on Mechatronics*, 29(4):2803–2811, 2024.

[6] Gang Li and Weidong Zhu. Experimental investigation on control of an infinitely variable transmission system for tidal current energy converters. *IEEE/ASME Transactions on Mechatronics*, 26 (4):1960–1967, 2021.

[7] Gang Li and Weidong Zhu. Design and power loss evaluation of a noncircular gear pair for an infinitely variable transmission. *Mechanism and Machine Theory*, 156:104137, 2021.

[8] Gang Li, Xuefeng Wang, and Weidong Zhu. Theoretical and experimental investigation on an integral time-delay feedback control combined with a closed-loop control for an infinitely variable transmission system. *Mechanism and Machine Theory*, 164:104410, 2021.

[9] Zhichang Qin, Gang Li, Weidong Zhu, and William Mayfield. Hierarchical speed control of an infinitely variable transmission in tidal current energy converters using integral reinforcement learning. *Ocean Engineering*, 328:121068, 2025.

[10] Mohammad Modarres, Mark P Kaminskiy, and Vasiliy Krivtsov. *Reliability engineering and risk analysis: a practical guide*. CRC press, 2016.

[11] Wen-Chi Cheng, Gang Li, and Mucun Sun. Probabilistic physics-of-failure based reliability assessment for an infinitely variable transmission. *Abstract Accepted in Probabilistic Safety Assessment and Management PSAM 18*, 2026.

[12] U Bhardwaj, AP Teixeira, and C Guedes Soares. Reliability prediction of an offshore wind turbine gearbox. *Renewable Energy*, 141:693–706, 2019.

[13] Artur Bejger, Ewelina Frank, and Przemys law Bartoszko. Failure analysis of wind turbine planetary gear. *Energies*, 14(20):6768, 2021.

[14] S Faulstich, B Hahn, P Lyding, and P Tavner. Reliability of offshore turbines–identifying risks by onshore experience. *Proc. of European Offshore Wind*, 69, 2009.

[15] Julia Walgern, Katharina Fischer, Paul Hentschel, and Athanasios Kolios. Reliability of electrical and hydraulic pitch systems in wind turbines based on field-data analysis. *Energy Reports*, 9: 3273–3281, 2023.

[16] Dimitri V Val, Leon Chernin, and Daniil Yurchenko. Updatable probabilistic evaluation of failure rates of mechanical components in power take-off systems of tidal stream turbines. *Energies*, 14 (20):6586, 2021.

[17] OP Gandhi, VP Agrawal, and KS Shishodia. Reliability analysis and evaluation of systems. *Reliability Engineering & System Safety*, 32(3):283–305, 1991.